IJRCS

International Journal of Robotics and Control Systems
Vol. 5, No. 1, 2025, pp. 105-123
ISSN 2775-2658
http://pubs2.ascee.org/index.php/ijrcs

ASCEE

Development of a Testbed for Autonomous Navigation of an Off-Shelf Quadrotor Based on Ultra-Wide-Band Real-Time Localization

Nelson Muchiri Gachoki [a,1,*], Stanley Kamau [a,2], Bernard Ikua [b,3]

[a] Department of Electrical and Electronic Engineering, Jomo Kenyatta University of Agriculture and Technology; Nairobi, Kenya
[b] Department of Mechatronic Engineering, Jomo Kenyatta University of Agriculture and Technology: Nairobi, Kenya
[1] mrgachoki@gmail.com; [2] skamau@eng.jkuat.ac.ke; [3] ikua_bw@eng.jkuat.ac.ke
[*] Corresponding Author

ARTICLE INFO

Article History
Received September, 30 2024
Revised November, 16 2024
Accepted December, 05 2024

Keywords
Autonomous Navigation;
Quadrotor;
Real-Time Localization Systems;
UAV Test-Bed;
Multi-Agent Systems;
Ultra-Wide-Band

ABSTRACT

Recent advances in autonomous aerial vehicle research, from theoretical simulations to experimental validations, has triggered demand for reliable proof-of-concept test-beds. Although such test-beds have been developed in some advanced drone research laboratories, their cost, expertise and complexity place them out of reach for upcoming research teams. This raises the need for development of less complex and affordable testbeds for quadrotor research. The contribution of this research is provision of low-cost autonomous quadrotor test-bed for proof-of-concept. The development of the proposed testbed entails configuration of Ultra-Wide-Band (UWB) based Real-Time Localization System (RTLS) to transmit position data of multiple agents to LabVIEW software for analysis and decision making. The autonomous navigation commands for the quadrotor are generated from the LabVIEW software and relayed through customized USB interface to the flight control module. The commands alter the digital state of Arduino board pins which are connected to the flight controller hence manipulating navigation pitch and roll parameters. The validation tests performed in the test-bed involved quadrotor hover and navigation in pursuit of the ground agent. The results demonstrate that UWB based RTLS achieves high precision of 99% when the modules are stationary but the precision reduced to 90% when the modules were in motion, which may be attributed actuating signal transmission delays. The results also showed that the Arduino based electronic flight controller is capable of generating flight paths to follow the ground robot in real-time with precision deviations of under 10% which is at par with other research test beds. This novel testbed provides a cost-effective and accurate solution for autonomous flight testing, with precision comparable to visual-based testbeds, but at a much lower cost. Further research is encouraged to explore how the system performs with more than two agents and on a wider test arena.

1. Introduction

Applications of multiagent robot systems has recently gained popularity, where a collection of robots work collaboratively in complex tasks beyond the capability of a single robot [1]–[3]. These

systems are widely applied in a number of civilian fields including rescue operations, collaborative search, surveillance, and exploration as evident in [4]–[6]. Researchers involved in development of autonomous multiagent system require proof-of-concept test-beds to transition their design to real-life applications.

Although the testbeds are crucial tools for advancements in aerial robotics, they comprise a vast amount of specialized software and hardware, necessitating extensive competence in computers and test hardware configurations [7]. These factors might slow down research and impede innovation, consequently the motivation for this paper is to promote further investigation in multiagent aerial robotics by creating a low cost easy deployment autonomous quadrotor navigation platform for proof-of-concept.

The composition of different agents in a multiagent system is dependent on envisioned application. The focus of this paper is on applications involving quadrotor class of Vertical Take-Off and Landing (VTOL) vehicles as aerial agents in active engagement of moving ground agents. Quadrotors have evolved into significant platforms for Unmanned Aerial Vehicle (UAV) research [8], [9]. Widespread preference of quadrotors in research is due to their simple mechanical systems, agility, availability, compact size, and affordability [10], [11]. They are best suited for research in environment monitoring, security surveillance, and pursuit among other uses [12]–[14]. With increase in applications of UAVs, is increasing demand for multiple heterogeneous agents for complex tasks beyond capabilities of a single agent. Positioning of the multiple agents and generation of multiple navigation paths are other research challenges in multiagent systems [2], [15], [16].

Pioneer researchers in multiagent testbeds in MIT, developed the Real-time indoor Autonomous Vehicle test ENvironment (RAVEN) a testbed for the rapid prototyping of UAVs [17]. Another multiagent platform developed at ETH Zurich is the Flying Machine Arena (FMA) [11].

Both the RAVEN and FMA consisted of high resolution cameras and relied on optical motion capture for determination of vehicle's position and orientation, hence best suited for obstacle free environment. While the RAVEN and FMA set a benchmark for future testbed development and provided acceptable results, the expertise required for their operation and the cost of components involved, hindered adoption of RAVEN at wide scale. Furthermore, their setting up requires a team of experts for multiple camera positioning and orientation and complex algorithms for vision data fusion, these are limitations associated with vision-based positioning systems [7], [18]. Generally vision based system have been found to have accuracy issues in environments with varying light intensity, they are also known to have high computational cost, since they work with real-time pattern recognition which require more computing memory and processing power [19].

Besides the works highlighted above, there are other platforms utilised in research, such as the Stanford's STARMAC [20], [21] and Upenn GRASP lab [22] which are dedicated labs. A different perspective is used in [23] where a low cost quadrotor testbed was developed, utilising AR.Drone and a personal computer, similar approach was adopted in [24].

To address the drawbacks of vision-based positioning systems such as limited range, high cost, computational complexity and required expertise, this research focuses on development of a more affordable solution, that is a Ultra-Wide-Band (UWB)-based flight validation testbed.

Previous applications of UWB technology in research, shows that the technology is simpler, cheaper, has lower computational requirement than vision based systems and provides stable positioning [25]–[27]. Hence this research proposes a testbed with a simpler set-up and lower computation requirements.

The main contributions of this paper is in the development and experimental evaluation of UWB based RTLS by integrating LabVIEW software, UWB modules and Arduino board resulting in a low-cost, scalable autonomous quadrotor navigation platform for proof-of-concept. In this work,the

testbed is built using UWB modules for positioning and open hardware Arduino based board for actuation. Processing is done using LabVIEW software on a Windows™computer. Whilst the proposed system offers high accuracy for two dimensional operations it may suffer diminished precision in z-axis, this is a common limitation of UWB based systems [28]. Future research on integration of UWB with more precise z-axis sensors might help overcome these limitations.

2. Features of Multiagent Testbed

2.1. General Architecture

The basic structure of a typical multiagent testbed has elements pertaining to both hardware and software. The core hardware components are the aerial vehicles, ground vehicles and the positioning system. The software in the ground computers is for processing of system's commands and for communicating to ground computers using communication protocols. Some testbeds such as [17] and [29], have integrated both aerial vehicles and ground agents.

The positioning systems used in most indoor applications are vision based, deploying multiple camera system to acquire positions of vehicles in an arena. For example the RAVEN has a high precision visual based system, Vicon MX motion-capture system [17]. Another desirable element of testbeds is wireless communication protocol, the typical 2.4GHz based wireless protocols are sufficient for most short range communication between the agents in the arena.

A flexible graphical interface is another important element necessary in the testbed. Vehicle data acquisition (DAQ) system is important feature of the testbed where vehicle data is acquired, transmitted and processed in the ground computer.

2.2. Hardware Features

The main UAV in the RAVEN testbed is a small and lightweight Draganflyer™V Ti-Pro quadrotor with a rechargeable battery sufficient for about 15 minutes flight. In the ETH Zurich's flying machine arena, Hummingbird quadrotor developed by Ascending Technologies is used [30].

The flight duration of hummingbird varies with the weight of the attached payload and can last up to thirty minutes [31]. Several other quadrotors have been applied in research such as the Parrot AR Drone quadrotor and X4 flyers as discussed in [24], [32]. The primary considerations in choice of quadrotor are design simplicity, flight duration and wireless communication capabilities [30].

2.3. Principles of UWB Positioning

UWB Technology is a Radio Frequency ranging defined by IEEE 802.15.4a standard and operating at high frequencies. The FCC describes UWB signal as having a bandwidth exceeding 500 MHz or a relative bandwidth of more than 20% of the central frequency [33], [34]. UWB offers sub-metre precision for shorter distances as compared to GNSS, which makes UWB ranging an excellent choice in indoor positioning systems [35], [36]. UWB is preferable to other Radio frequency (RF) ranging technologies such as ZigBee and Bluetooth Low Energy(BLE), due to its broader range and ability to resist multipath interference and high material penetrability [37]. A detailed analysis of all the other indoor localization systems and comparison with UWB was done in [38]–[40].

Since UWB relies on multilateration for position determination, it utilizes geometric algorithms for timing of signal transmissions between sensors. Such algorithms include; Time of Arrival (TOA), Time Difference of Arrival (TDOA), two-way Time-of-Flight (TOF), Angle of arrival (AOA) and Received Signal Strength Indication (RSSI) [35], [41].

RSSI, TOA, TOF and TDOA are lateration based algorithms, where RSSI relies on signal strength and TOF, TDOA, TOA are based on propagation time [42]. TDOA requires time synchronization and is affected by multipath effects which may lead to a decline in localization accuracy, while RSSI al-

gorithm is sensitive to environment and interferences from other wireless devices [43]. The principle behind RSSI is that signal power decreases as the distance between the Transmitting Node (TN) and the Responding Node (RN) increases [44]. TOA is based on the propagation time, which is directly proportional to the distance between RN and TN [45]. The DWM1001DEV Modules deployed in this research are based on two way TOF. The two-way TOF scheme is shown in Fig. 1.

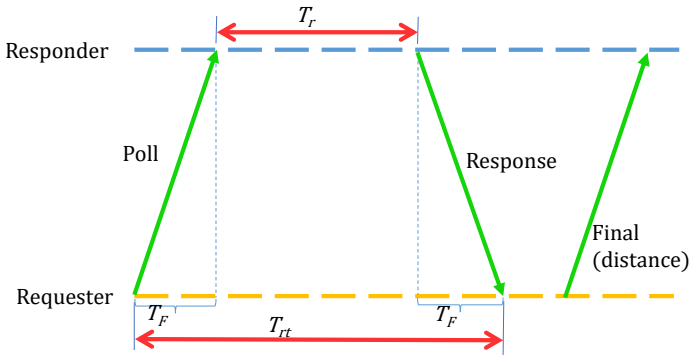

Fig. 1. Two-Way ranging scheme

The range R (distance between requester and responder) is computed from Eq (1).

$$R = \frac{T_{rt} - T_r}{2} c \tag{1}$$

where:-

c is the speed of light.
T_F is Time of Flight.
T_r is time taken by the responder to process poll signal.
T_{rt} is the overall time taken from when the poll is sent to when the response is received.

For a two-dimensional arena, precise position is obtained using UWB based trilateration. By obtaining known distances from a specific points where anchors are located and application of geometric principles, the position of each point can be identified. [46]. GNSS systems use this principle with multiple satellites, and so does cellphone base-transceiver towers [47].

For a two-dimensional space, only three locations are needed, hence the name "Trilateration". Fig. 2 illustrates trilateration where three beacons B_1, B_2 and B_3, whose locations are known in the coordinate system, are references to target T of an unknown location.

The distances from the target to each beacon (d_1, d_2,and d_3,) can be obtained using the UWB ranging sensor, and the x,y position of the target is determined in Equations (2)–(4).

$$d_1^2 = (x - x_1)^2 + (y - y_1)^2 \tag{2}$$

$$d_2^2 = (x - x_2)^2 + (y - y_2)^2 \tag{3}$$

$$d_3^2 = (x - x_3)^2 + (y - y_3)^2 \tag{4}$$

In Equations (2)–(4), x and y positions are obtained in Equation (5) and (6) respectively.

$$x = \frac{(d_2^2 - d_1^2 + x_1^2 - x_2^2 + y_1^2 - y_2^2)(2y_3 - 2y_2) - (d_2^2 - d_3^2 + x_3^2 - x_2^2 + y_3^2 - y_2^2)(2y_1 - 2y_2)}{(2y_3 - 2y_2)(2x_1 - 2x_2) - (2y_1 - 2y_2)(2x_3 - 2x_2)} \tag{5}$$

$$y = \frac{(d_2^2 - d_1^2 + x_1^2 - x_2^2 + y_1^2 - y_2^2)(2x_3 - 2x_2) - (d_2^2 - d_3^2 + x_3^2 - x_2^2 + y_3^2 - y_2^2)(2x_1 - 2x_2)}{(2y_1 - 2y_2)(2x_3 - 2x_2) - (2y_3 - 2y_2)(2x_1 - 2x_2)} \tag{6}$$

Equation (5) and (6) generate the exact target coordinates (x,y) provided all other nine parameters(x_1, y_1, d_1, x_2, y_2, d_2, x_3, y_3 and d_3) are known. Whereas UWB is a relatively new positioning technology,

it has received significant attention in research community, for example in [33] where it was coupled with Global Positioning System (GPS) for operation in both indoor and outdoor environment. The works of Ruiz and Granja [48], evaluated the commercial UWB systems from DecaWave, Ubisense and BeSpoon in an industrial testing space, concluding superior performance of Decawave's modules. This, and further research by Jiménez and Seco [49], informed the choice of the modules used in this research.

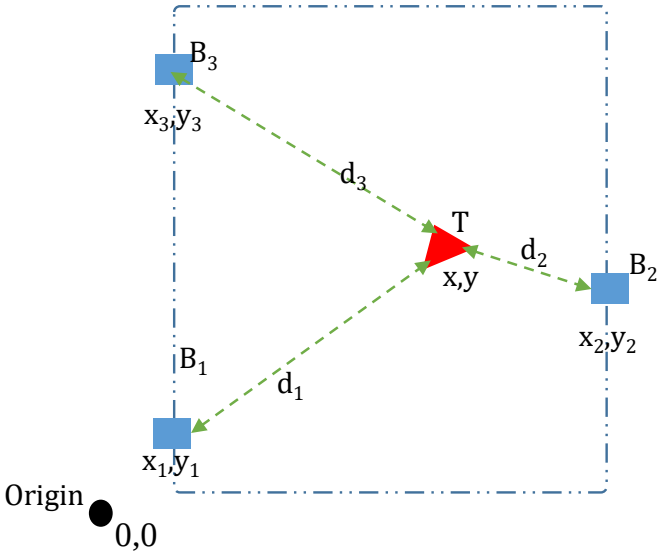

Fig. 2. Trilateration

2.4. Principles of Quadrotor Flights

Quadrotors utilize four rotors in a cross layout to produce varying manoeuvres with six degrees of freedom from four inputs, hence are categorized as under-actuated systems [9], [50]. The propellers attached to the arms of the quadrotors create torque in the opposite direction of rotation and a force perpendicular to the rotational plane as illustrated in Fig. 3.

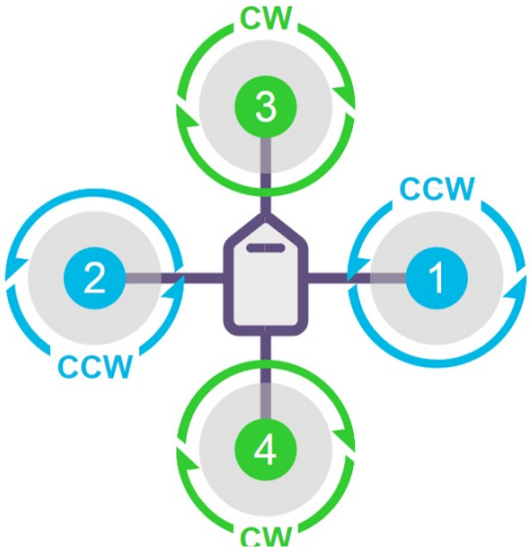

Fig. 3. Cross configuration [51]

From the illustration in Fig. 3, rotor 1 and rotor 2 move in counter-clockwise direction, while rotor 3 and rotor 4 move in the opposite direction (clockwise). Adjusting the rotor speed dictates the roll, pitch, yaw, and upward thrust movements to achieve the intended results [52].

The movement of the quadrotor is determined by the actuating signals as shown in the simplified model shown in equations (7)–(11).

$$u_1 = b(\Omega_1^2 + \Omega_2^2 + \Omega_3^2 + \Omega_4^2) \tag{7}$$

$$u_2 = b(\Omega_3^2 - \Omega_4^2) \tag{8}$$

$$u_3 = b(\Omega_2^2 - \Omega_1^2) \tag{9}$$

$$u_4 = b(\Omega_1^2 - \Omega_2^2 + \Omega_3^2 - \Omega_4^2) \tag{10}$$

$$\Omega_r = \Omega_2 + \Omega_4 - \Omega_1 - \Omega_3 \tag{11}$$

where b represents the quadrotor's parameters such as weight, u_1, u_2, u_3, and u_4 are the four inputs and $\Omega_i \in \mathbb{R}, i = \ldots, 4$ are the resulting rotor speeds.

The control signal u_1, is throttle, increase in throttle results to all propeller speeds increasing at the same rate, hence the quadrotor moves upwards. Likewise, decrease in throttle results in quadrotor moving downwards. Signal u_2 controls the pitch and forward/reverse movement. Increasing the magnitude of signal u_2, causes the speed of propeller 3 (Ω_3) to increase and that of propeller 4 (Ω_4) to decrease hence the quadrotor moves backwards. Decreasing the magnitude of signal u_2, causes the speed of propeller 3 (Ω_3) to decrease and that of propeller 4 (Ω_4) to increase hence the quadrotor moves forward. In the same manner, signal u_3 manipulates the roll and side-ways movement; when signal u_3 is increased, the speed of rotation of propeller 2 (Ω_2) is increased and that of propeller 1 (Ω_1) is decreased, resulting right-ward movement of the quadrotor. In the same manner, decreasing signal u_3, reduces the speed of rotation of propeller 2 (Ω_2), and increases that of propeller 1 (Ω_1), resulting in left-ward movement of the quadrotor. The yaw, that is the orientation of the quadrotor is controlled by signal u_4. When signal u_4 is increased, the difference between the speeds of opposite propellers changes according to (10) hence the quadrotor rotates.

3. Methodology

A summary of the research methodology utilized in this paper is illustrated in the flowchart in Fig. 4. Based on the analysis of testbeds in the literature surveyed, it was observed that, generally a testbed should consist of at least a positioning system, an aerial vehicle and processing computer. In developing the proposed testbed, a similar design approach is used, where the positioning system is interconnected with a computer and an actuating system. The testbed architecture is shown in Fig. 5.

For the ground control station, a standard laptop computer with Windows™ operating systems was used. LabVIEW software was used to carry out the commands and data acquisition. LabVIEW was chosen for its reliable interface with data acquisition hardware and flight control hardware, as well as the ease of development of interface design [29], [53]. For the quadrotor, most off-shelf FPV (First Person View) quadrotors in the market would do. In this research, the Snaptain™ S5C Wi-Fi FPV Quadrotor was preferred for its low cost, robustness and its navigation circuit easy to modify. The modifications on the joystick controls are highlighted in the next section.

3.1. Quadrotor Modifications

Due to stringent weight constraints of the quadrotor, not much additional weight can be added without altering its flight dynamics. This poses a challenge when positioning has to be onboard during flight. To overcome this, the approach taken in this research was substitution of the original camera payload of the quadrotor with the sensor payload. This entailed removing the quadrotor's detachable

video camera of about 30 grams, and in its place connecting the UWB module as shown in Fig. 6. The board, with its casing removed weight is 15 grams.

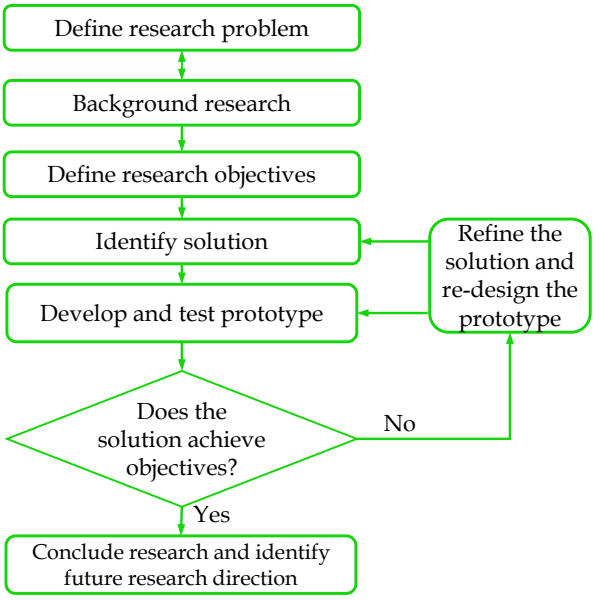

Fig. 4. Research methodology

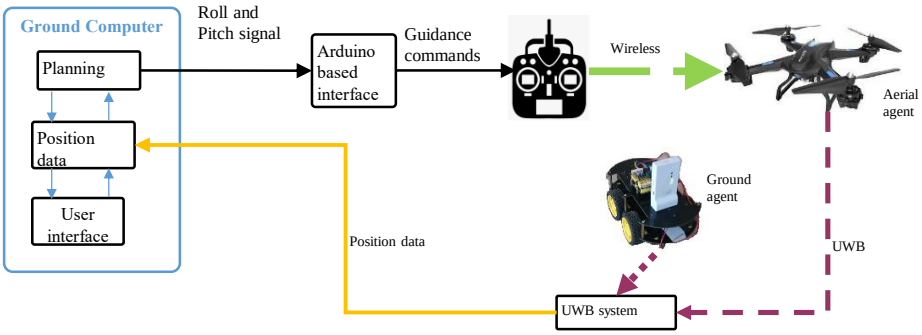

Fig. 5. Hardware architecture

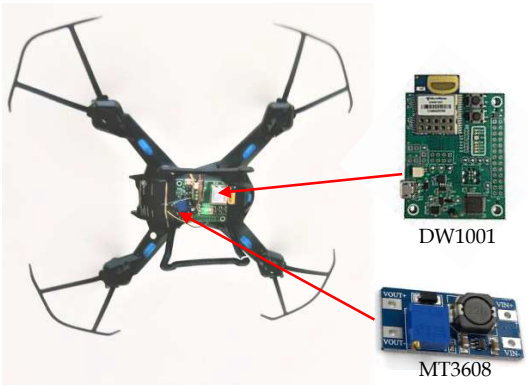

Fig. 6. Snaptain quadrotor with MT3608 and DWM1001DEV modules

The board was powered using the camera socket. An MT3608 switch mode DC-DC boost converter was added to provide a stable power supply to the board. These modifications did not change the overall weight of the quadrotor and the flight dynamics. The MT3608 module has a two Ampere step up converter, that can convert very low voltages from 2V to higher DC voltages of up to 28V [54]. This resulted to a very stable 5V supply to the sensor board.

3.2. Modifications of the Control Circuit

The Snaptain quadrotor is an off-shelf drone designed for hobbyist. The quadrotor's flight navigation commands are sent wirelessly from the remote control module. The remote control module, is essentially a 2.4GHz radio transmitter with two joystick modules. The operation of the joystick modules was modified to enable automatic flight control from the computer.

The joystick converts the angle of the operating shaft to a voltage signal, proportional to the inclination of the shaft. The variations on the position of the operating shaft, varies the resistance of the internal potentiometer hence turning its displacement into an electrical voltage signal. Based on the connections to the control microprocessor, the voltage signal affects the Roll, the Pitch, the Yaw or the Throttle of the quadrotor.

An external circuit based on Arduino UNO was created to generate equivalent voltages to depict the desired Roll, Pitch, Throttle and Yaw signals. Fig. 7 shows the circuit schematic of the circuit.

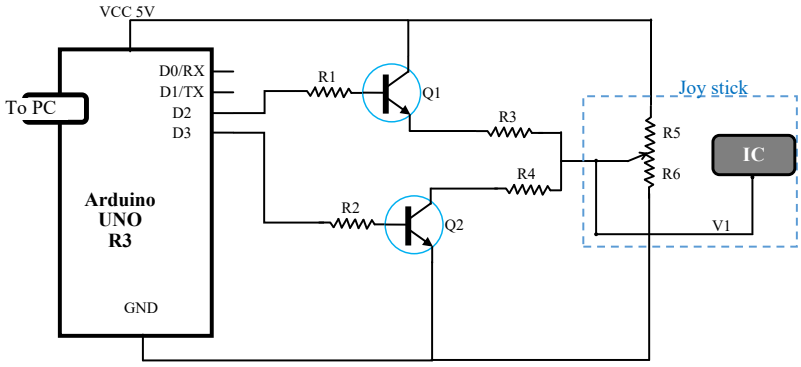

Fig. 7. Circuit schematic

In the schematic diagram, Fig. 7. The resistors R_5 and R_6 are the two parts of the internal potentiometer of the joystick. The movement of the joystick alters the ratio R_5:R_6 hence the voltage V_1. From the voltage divider principle, the voltage V_1 to the IC is described in Eq (12).

$$V_1 = \left(\frac{R_6}{R_5 + R_6} \right) \times 5V \tag{12}$$

Transistors Q_1 and Q_2 are connected as switch in a form of push-pull mode, where Q_1 pushes up the voltage and Q_2 pulls down. The transistors are driven to saturation or cut-off by the action of Arduino digital pins D_2 and D_3. Since Arduino UNO's digital pins are directly manipulatable form computer using LabVIEW's LINX interface, therefore the flight parameters could be controlled directly from the computer.

The operation of the system is such that if both D_1 and D_2 are Low, there is no change in voltage V_1 and the joystick output remains at $\simeq$ 1.7 Volts. When D_2 is High and D_3 is Low, transistor Q_1 is driven to saturation while Q_2 is still in cut-off. This places R_3 in parallel with R_5, the voltage V_1 then

is as defined by equation (13).

$$V_1 = \left(\frac{R_6}{\frac{R_3 \times R_5}{R_3 + R_5} + R_6} \right) \times 5V \tag{13}$$

The value of V_1 in equation (13) is higher than that of V_1 in equation (12) hence drives the voltage to the IC to a higher value. When D_3 is High and D_2 is Low, Q_2 is driven to saturation while Q_1 is in cut-off, this places resistor R_6 in parallel with R_4 hence drives the voltage V_1 to a low value as expressed in equation (14).

$$V_1 = \left(\frac{\frac{R_4 \times R_6}{R_4 + R_6}}{\frac{R_4 \times R_6}{R_4 + R_6} + R_5} \right) \times 5V \tag{14}$$

Therefore it is the values of R_3 and R_4 that determine how high or low the voltage V_1 goes. The computer code that controls the switching is made in a way that both switches cannot be high at the same time since this might damage the transistors. The actuating signal is generated from the computer LabVIEW code and channelled through LINX interface shown in Fig. 8.

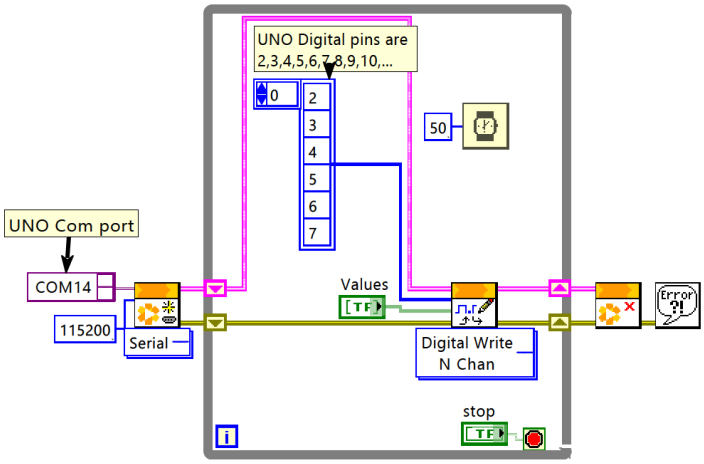

Fig. 8. LINX arduino control interface

This code defines the computer's serial port being used for transmission of the actuation signals (COM14) and the Baud rate for data transfer. It also defines the digital output pins of the Arduino UNO and writes the Boolean values to the digital pins.

3.3. Position Data Acquisition

The position of the Quadrotor and the ground vehicle was determined using Qorvo ™ (*Decawave*) RTLS modules (DWM1001) positioning system. The system has modules which can be configured as anchors or tags. Anchors should be positioned stationary in the environment as beacons, whereas nodes set as tags are utilized on the device whose location is of interest. In the experiment set-up, the four anchor modules were placed in a rectangular obstacle free room of 7.7 metres by 13.5 metres, in a non-symmetric arrangement as in Fig. 9.

One of the anchor module was configured as the initiator (reference module), by which all other modules' positions were configured. Two modules were configured as tags, where one was attached to the ground agent and the other was attached to the quadrotor. Another module was configured as a listener, for purpose of transmitting the states of the other tags to the computer.

Fig. 9. Anchor positions in arena

The listening module was interfaced to the computer through USB serial port and position data acquired using Tera-term software. This data is then processed in real-time using LabVIEW. Fig. 10 shows a screenshot of the Tera-term data acquisition interface during tests.

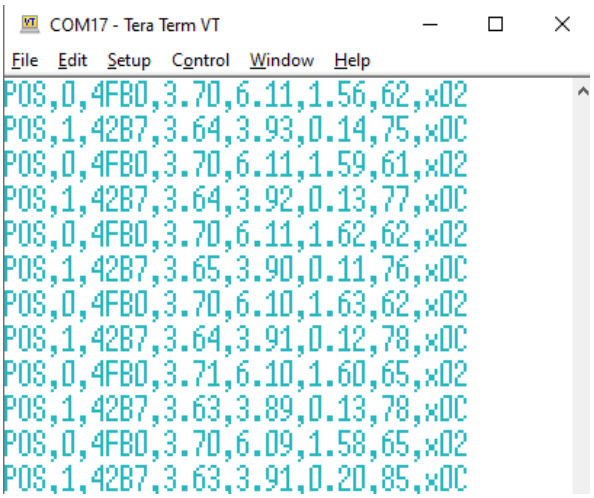

Fig. 10. Tera-term screenshot

The data is in form of comma separated values (CSV) making it easy to filter by a computer program. The first three values in each line, identify the module whose location data is being handled. In this case there are two modules (0 and 1) whose ID is 4FB0 and 42B7 respectively.

The next three CSV are indicators of position in X, Y and Z coordinate system. For example the first value shows that module 4FB0 (0) is 3.7 metres from the origin along X axis, 6.11 metres along

Y axis and 1.56 metres from the ground. The last field of the line is a number (62), which is "quality factor", when this value is near 100 indicates good quality, whereas less than 50 indicates bad quality on a scale from 0 to 100 [49].

The position data from serial port was then parsed to LabVIEW for processing. The proposed system functions as illustrated in the flow chart in Fig. 11.

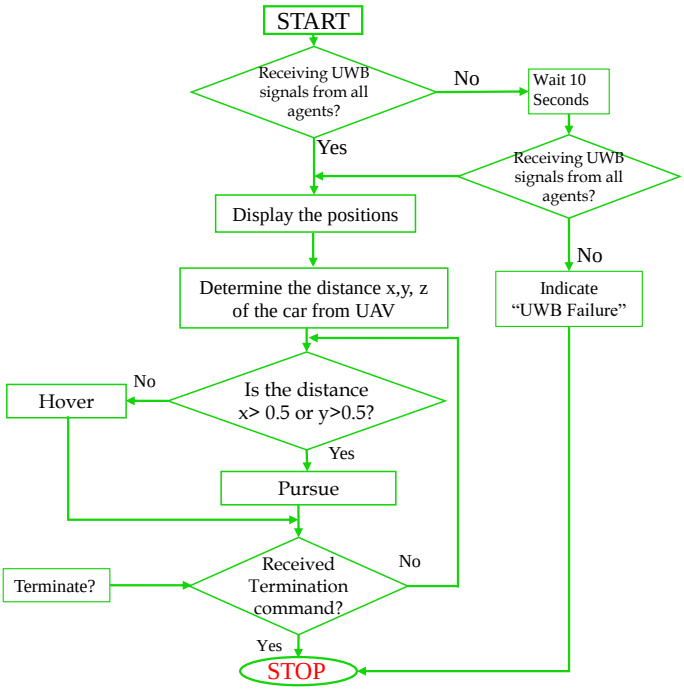

Fig. 11. System flow chart

The program begins execution at START, then determines if UWB signals are being received from both the robot-car and the quadrotor UAV. If the signals are being received, the program determines the locations otherwise it indicates signal reception error. After determining the location of the robot-car, pursuit begins if the robot-car is more than 0.5 meters from the UAV on x or y direction. This is executed over and over until the terminating command is received.

4. System Test Evaluation (Results and Discussions)

4.1. Static Precision

Assessment of static precision is essentially the first step in evaluation of a localization technique, so the DWM1001 UWB receiver module was placed in a stationary position (4,5,1) for three minutes to collect position data samples. The outcomes of a two-dimensional stationary scatter over a span of three minutes and the distribution percentages are shown in Fig. 12.

Part (a) of Fig. 12 has the location of the points on the plane while parts b and c show the percentage of deviations of locations from the actual along the x and the y axis.

From the results in Fig. 12 (a), the mean error on the x axis is 0.03151metres and on the y axis is 0.00813metres, with a maximum deviation of 0.11metres along x axis and 0.05metres along y axis. Furthermore it is evident that over 99% of the points in $x - y$ plane are within 10cm of the desired point, implying high precision. The random stray points, could be due to errors attributed to the tag orientation or proximity of the tag to an anchor, this could be mitigated by use of additional anchors. The obtained static results are in agreement with results obtained by Dotlic et al [55]. and Delamare

et al [56] who used Decawave UWB modules and obtained static mean errors of 1cm. The UWB's high static accuracy is also comparable with that of visual based systems with mean error of 1cm in [11] and [17].

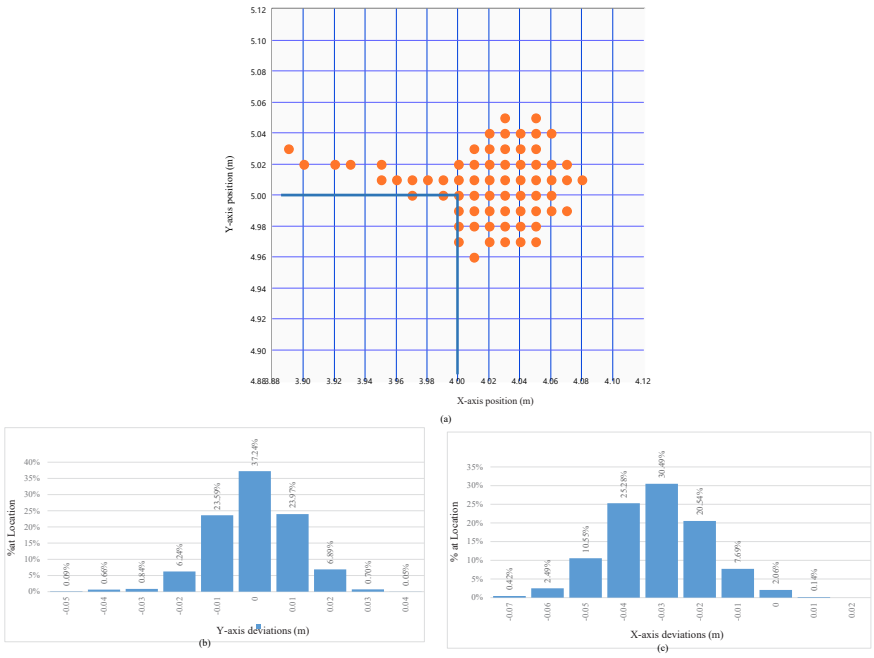

Fig. 12. Static precision map

4.2. Evaluation of Precision During Hover

The hover test evaluates how well the proposed system can maintain the quadrotor's position during flight. This is an indication of how swiftly the sensor acquires data, transmits that data to the computer and that data is processed resulting to actuation commands. In this test, the Snaptain quadrotor was commanded to hover within 1 metre of (x, y, z : 4, 5, 1) m for three minutes. Three minutes duration was chosen since beyond this period, the quadrotor's performance degrades due to low charge of the battery. One metre allowance was chosen to allow for time for the computer to process commands.

The results for $x - y$ plot of the quadrotor are shown in Fig. 13. The thick blue rectangular line indicates the region which the quadrotor is expected to remain within, that is 1 metre from (4, 5, 1). The histogram for quadrotor percentage of time at location for x and y are shown in Fig. 14.

It is evident from Fig. 13 and Fig. 14 that for the longer percentage duration, the quadrotor remains within the expected region. From these results, it is evident that the system is capable of maintaining a steady quadrotor's position during flight.

4.3. Evaluation of Tracking Precision

In order to evaluate how well the system can track a moving ground target, the robot-car was made to move in a perfect circle of diameter 3.5 metres. The results are as shown in Fig. 15. In Fig. 15, the blue dots are the perfect circle which the robot-car was made to move in, the green dots are the robot-car path data as acquired by the UWB RTLS. The anchors' locations in the arena are also shown. It was observed from the generated path that UWB tracks the circular path successfully with very minimal deviations. These results are consistent with the findings of [44] in UWB tracking experiment.

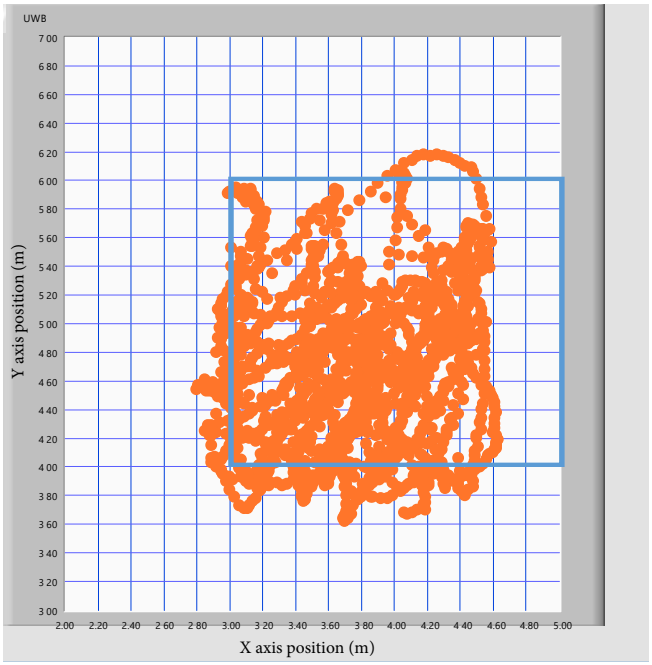

Fig. 13. Hover locations x and y

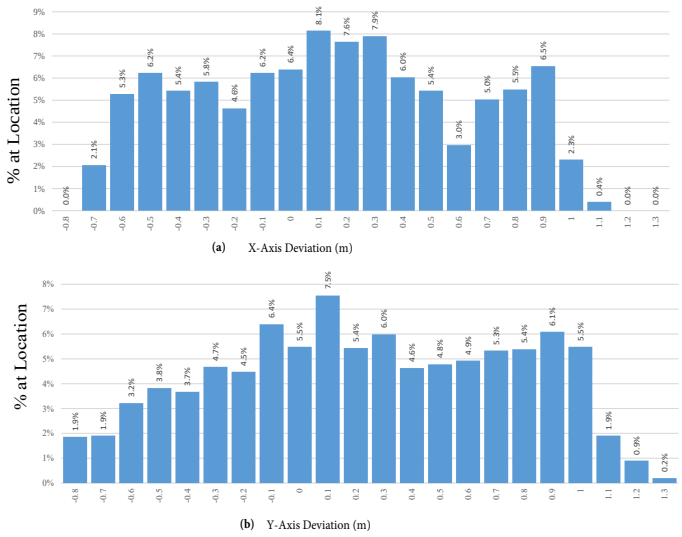

Fig. 14. Deviations during hover for x and y

It is observed that although the car moves in a perfect circle, the points plotted are not perfectly circular but oscillate. This could be attributed to the precision of UWB modules which is affected by signal strength or tag orientation. Another observation is the presence of distortions in the UWB acquired path data around points x, y 4.5, 4 of Fig. 15. The tag signal does not form a perfect circle, the cause of this should be investigated further considering UWB is affected by multipath transmission.

The Snaptain quadrotor was made to track the robot-car as the robot-car moved round the circle. The results are as shown in Fig. 16. In Fig. 16, the blue dots are the robot-car path as measured by the UWB RTLS, while the orange dots shows the quadrotor tracking the robot-car as it moved. The anchors' locations in the arena are also shown.

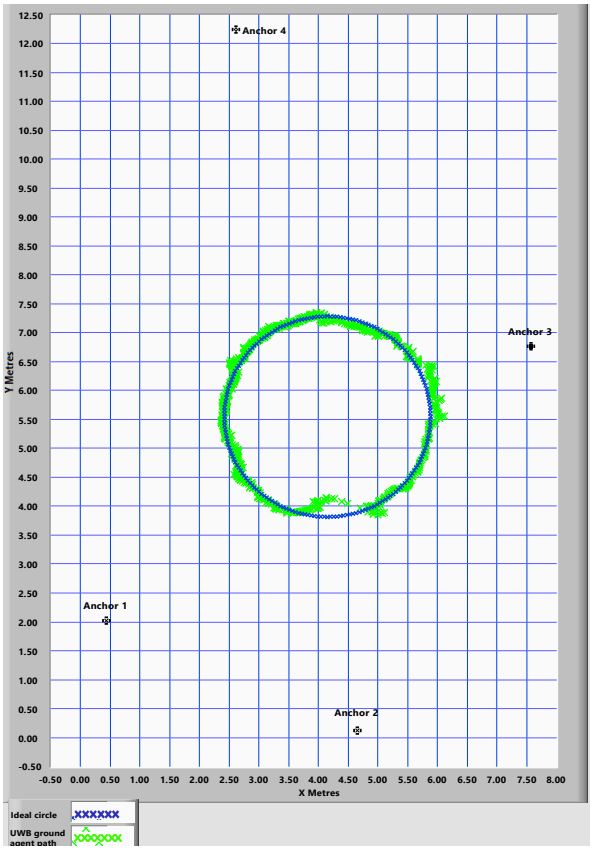

Fig. 15. Tracking a circle

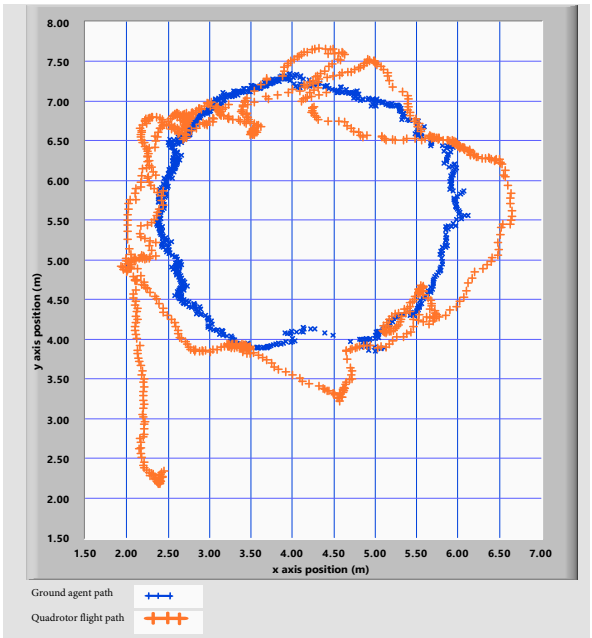

Fig. 16. UAV following robot car

The Real-time path samples for both the robot-car and the quadrotor for one complete circle along x direction are as shown in Fig. 17 and in y direction in Fig. 18. The blues plot of Fig. 17 is the variation of the robot-car along x axis while the orange line is the variations of the quadrotor along

x axis as it follows the robot-car. The Standard deviation along x-axis was determined as 0.173m and along y-axis was determined as 0.621m. These results are in agreement with results obtained in similar conditions in [56], where the standard deviation in x-axis was 0.18m and y-axis was 0.00m.

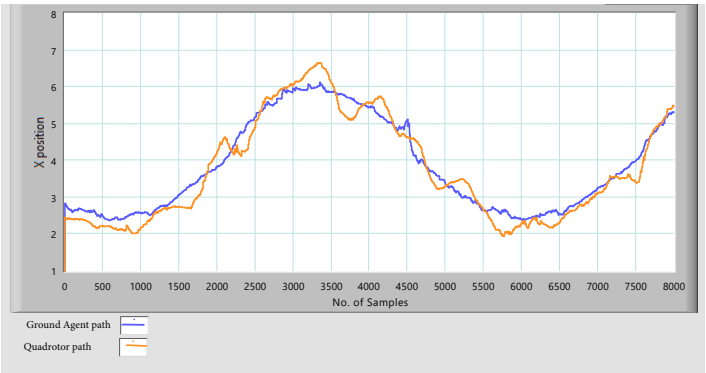

Fig. 17. Path deviation along X-axis

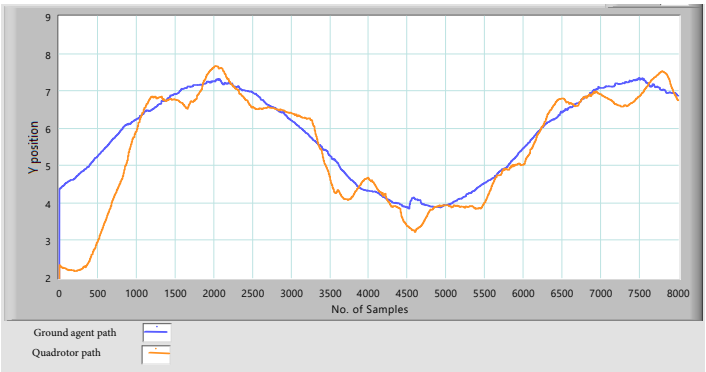

Fig. 18. Path deviation along Y-axis

It can be seen from Fig. 16, Fig. 17, and Fig. 18 that the system can effectively track a ground target. The results demonstrate that the system maintains the pursuing quadrotor within 1 metre of the ground target throughout the entire test flight. Whereas the results are acceptable for general applications, they are not as fine as was achieved by [24], who utilized a filter in a GPS based system to achieve a more consistent tracking.

5. Conclusions and Recommendations

A UWB based proof-of-concept test environment for autonomous quadrotors was developed for evaluation of pursuit environment. The design entailed novel integration UWB RTLS with an off-shelf quadrotor and modification of quadrotor flight control for autonomous flights. The resulting system was tested with a single quadrotor and a single ground agents, although more agents would not alter its performance. It was observed that UWB provides high precision for localization system and updates position data fast enough for real-time decision making. This system however is limited to agents whose velocity is under $1m/s$ due to the UWB system low sampling rate of 10 frames per second and accuracy of 0.1 metres, this however could be overcome in future system by improving sampling rate of UWB modules or integrating the UWB system with a visual based systems of 200 frames per second. This would make the system suitable for fast moving multiagent system. The developed testbed offers a low cost high accuracy solution for autonomous flight test whose reliability matches visual based testbeds developed by other researchers albeit at a significantly low cost. It may be of interest that further experiment with the system to include more than two agents and to increase

the number of anchors. Since the system has processing delays, including state estimation by Kalman filter may improve results in future design of the system.

Author Contribution: All authors contributed equally to this paper. All authors read and approved the final paper.

Funding: This research received funding from AFDB.
Conflicts of Interest: The authors declare no conflict of interest.

References

[1] F. Aljalaud, H. Kurdi, and K. Y. Toumi, "Bio-inspired multi-uav path planning heuristics: A review," *Mathematics*, vol. 11, no. 10, p. 2356, 2023, https://doi.org/10.3390/math11102356.

[2] Z. H. Ismail and N. Sariff, "A survey and analysis of cooperative multi-agent robot systems: Challenges and directions," in *Applications of Mobile Robots*, 2019, https://doi.org/10.5772/intechopen.79337

[3] J. Qin, Q. Ma, Y. Shi and L. Wang, "Recent Advances in Consensus of Multi-Agent Systems: A Brief Survey," in *IEEE Transactions on Industrial Electronics*, vol. 64, no. 6, pp. 4972-4983, 2017, https://doi.org/10.1109/TIE.2016.2636810.

[4] D. S. Drew, "Multi-agent systems for search and rescue applications," *Current Robotics Reports*, vol. 2, no. 2, pp. 189–200, 2021, https://doi.org/10.1007/s43154-021-00048-3.

[5] L. Han, W. Song, T. Yang, Z. Tian, X. Yu, and X. An, "Cooperative decisions of a multi-agent system for the target-pursuit problem in manned–unmanned environment," *Electronics*, vol. 12, no. 17, p. 3630, 2023, https://doi.org/10.3390/electronics12173630.

[6] R. Rahimi, F. Abdollahi, and K. Naqshi, "Time-varying formation control of a collaborative heterogeneous multi agent system," *Robotics and autonomous systems*, vol. 62, no. 12, pp. 1799–1805, 2014, https://doi.org/10.1016/j.robot.2014.07.005.

[7] T. Oliveira, P. Trindade, D. Cabecinhas, P. Batista and R. Cunha, "Rapid Development and Prototyping Environment for Testing of Unmanned Aerial Vehicles," *2021 IEEE International Conference on Autonomous Robot Systems and Competitions (ICARSC)*, pp. 191-196, 2021, https://doi.org/10.1109/ICARSC52212.2021.9429816.

[8] M. Maaruf, M. S. Mahmoud, and A. Ma'arif, "A survey of control methods for quadrotor uav," *International Journal of Robotics and Control Systems*, vol. 2, no. 4, pp. 652–665, 2022, https://doi.org/10.31763/ijrcs.v2i4.743.

[9] H. Mo and G. Farid, "Nonlinear and adaptive intelligent control techniques for quadrotor uav – a survey," *Asian Journal of Control*, vol. 21, no. 2, pp. 989–1008, 2018, https://doi.org/10.1002/asjc.1758.

[10] Lasmadi, F. Kurniawan, D. Dermawan, N. A. Purnami and R. Alriavindra Funny, "Simulation of Orientation Navigation Based on IMU Sensor for Quadrotor Using Kalman Filter," *2023 International Conference on Electrical and Information Technology (IEIT)*, pp. 76-81, 2023, https://doi.org/10.1109/IEIT59852.2023.10335574.

[11] S. Lupashin, M. Hehn, M. W. Mueller, A. P. Schoellig, M. Sherback, and R. D'Andrea, "A platform for aerial robotics research and demonstration: The flying machine arena," *Mechatronics*, vol. 24, no. 1, pp. 41–54, 2014, https://doi.org/10.1016/j.mechatronics.2013.11.006.

[12] M. Ghosal, A. Bobade and P. Verma, "A Quadcopter Based Environment Health Monitoring System for Smart Cities," *2018 2nd International Conference on Trends in Electronics and Informatics (ICOEI)*, pp. 1423-1426, 2018, https://doi.org/10.1109/ICOEI.2018.8553686.

[13] S. Berrahal, J.-H. Kim, S. Rekhis, N. Boudriga, D. Wilkins, and J. Acevedo, "Border surveillance monitoring using quadcopter uav-aided wireless sensor networks," *Journal of Communications Software and Systems*, vol. 12, no. 1, pp. 67–82, 2016, https://doi.org/10.24138/jcomss.v12i1.92.

[14] A. Basit, W. S. Qureshi, M. N. Dailey, and T. Krajník, "Joint localization of pursuit quadcopters and target using monocular cues," *Journal of Intelligent & Robotic Systems*, vol. 78, pp. 613–630, 2015, https://doi.org/10.1007/s10846-014-0081-2.

[15] A. Amirkhani and A. Barshooi, "Consensus in multi-agent systems: a review," *Artificial Intelligence Review*, vol. 55, pp. 1–39, 11 2021, http://dx.doi.org/10.1007/s10462-021-10097-x.

[16] P. T. Nathan, H. A. F. Almurib and T. N. Kumar, "A review of autonomous multi-agent quad-rotor control techniques and applications," *2011 4th International Conference on Mechatronics (ICOM)*, pp. 1-7, 2011, https://doi.org/10.1109/ICOM.2011.5937132.

[17] J. P. How, B. Behihke, A. Frank, D. Dale, and J. Vian, "Real-time indoor autonomous vehicle test environment," *IEEE Control Systems Magazine*, vol. 28, no. 2, pp. 51–64, 2008, http://dx.doi.org/10.1109/mcs.2007.914691.

[18] M. Y. Arafat, M. M. Alam, and S. Moh, "Vision-based navigation techniques for unmanned aerial vehicles: Review and challenges," *Drones*, vol. 7, no. 2, p.89, 2023, https://doi.org/10.3390/drones7020089.

[19] D. Khan, Z. Cheng, H. Uchiyama, S. Ali, M. Asshad, and K. Kiyokawa, "Recent advances in vision-based indoor navigation: A systematic literature review," *Computers & Graphics*, vol. 104, pp. 24–45, 2022, https://doi.org/10.1016/j.cag.2022.03.005.

[20] G. M. Hoffmann, H. Huang, S. L. Waslander, and C. J. Tomlin, "Precision flight control for a multi-vehicle quadrotor helicopter testbed," *Control engineering practice*, vol. 19, no. 9, pp. 1023–1036, 2011, http://dx.doi.org/10.1016/j.conengprac.2011.04.005.

[21] G. Hoffmann, D. G. Rajnarayan, S. L. Waslander, D. Dostal, J. S. Jang and C. J. Tomlin, "The Stanford testbed of autonomous rotorcraft for multi agent control (STARMAC)," *The 23rd Digital Avionics Systems Conference (IEEE Cat. No.04CH37576)*, pp. 12.E.4-121, 2004, https://doi.org/10.1109/DASC.2004.1390847.

[22] N. Michael, D. Mellinger, Q. Lindsey, and V. Kumar, "The grasp multiple micro-uav testbed," *IEEE Robotics & Automation Magazine*, vol. 17, no. 3, pp. 56–65, 2010, http://dx.doi.org/10.1109/mra.2010.937855.

[23] L. V. Santana, A. S. Brandao, M. Sarcinelli Filho and R. Carelli, "A Computational System for Trajectory Tracking and 3D Positioning of Multiple UAVs," *2014 Joint Conference on Robotics: SBR-LARS Robotics Symposium and Robocontrol*, pp. 118-123, 2014, https://doi.org/10.1109/SBR.LARS.Robocontrol.2014.22.

[24] L. V. Santana, A. S. Brandao, and M. Sarcinelli-Filho, "An open-source testbed for outdoor navigation with the ar.drone quadrotor," *IEEE Systems Journal*, vol. 15, no. 3, pp. 3597–3608, 2021, http://dx.doi.org/10.1109/jsyst.2020.3020012.

[25] G. Retscher *et al.*, "A benchmarking measurement campaign in gnss-denied/challenged indoor/outdoor and transitional environments," *Journal of Applied Geodesy*, vol. 14, no. 2, pp. 215–229, 2020, https://doi.org/10.1515/jag-2019-0031.

[26] P. Dabove, V. Di Pietra, M. Piras, A. A. Jabbar and S. A. Kazim, "Indoor positioning using Ultra-wide band (UWB) technologies: Positioning accuracies and sensors' performances," *2018 IEEE/ION Position, Location and Navigation Symposium (PLANS)*, pp. 175-184, 2018, https://doi.org/10.1109/PLANS.2018.8373379.

[27] W. You, F. Li, L. Liao, and M. Huang, "Data fusion of uwb and imu based on unscented kalman filter for indoor localization of quadrotor uav," *IEEE Access*, vol. 8, pp. 64971–64981, 2020, http://dx.doi.org/10.1109/access.2020.2985053.

[28] W. Chantaweesomboon *et al.*, "On performance study of UWB real time locating system," *2016 7th International Conference of Information and Communication Technology for Embedded Systems (IC-ICTES)*, pp. 19-24, 2016, https://doi.org/10.1109/ICTEmSys.2016.7467115.

[29] F. M. Palacios, E. S. E. Quesada, G. Sanahuja, S. Salazar, O. G. Salazar, and L. R. G. Carrillo, "Test bed for applications of heterogeneous unmanned vehicles," *International Journal of Advanced Robotic Systems*, vol. 14, no. 1, 2017, https://doi.org/10.1177/1729881416687111.

[30] W. T. L. Teacy, J. Nie, S. McClean, G. Parr, S. Hailes, S. Julier, N. Trigoni, and S. Cameron, "Collaborative sensing by unmanned aerial vehicles," in *Third International Workshop on Agent Technology for Sensor Networks (ATSN-09)*, p. 13, 2009, http://www.cs.ox.ac.uk/files/3063/atsn.pdf.

[31] D. Gurdan, J. Stumpf, M. Achtelik, K. -M. Doth, G. Hirzinger and D. Rus, "Energy-efficient Autonomous Four-rotor Flying Robot Controlled at 1 kHz," *Proceedings 2007 IEEE International Conference on Robotics and Automation*, pp. 361-366, 2007, https://doi.org/10.1109/ROBOT.2007.363813.

[32] E. B. Davis, *Aerodynamic force interactions and measurements for micro quadrotors*, PhD Thesis, School of Information Technology and Electrical Engineering, The University of Queensland, 2018, https://doi.org/10.14264/uql.2018.636.

[33] W. Jiang, Z. Cao, B. Cai, B. Li and J. Wang, "Indoor and Outdoor Seamless Positioning Method Using UWB Enhanced Multi-Sensor Tightly-Coupled Integration," in *IEEE Transactions on Vehicular Technology*, vol. 70, no. 10, pp. 10633-10645, 2021, https://doi.org/10.1109/TVT.2021.3110325.

[34] F. Zhang, L. Yang, Y. Liu, Y. Ding, S.-H. Yang, and H. Li, "Design and implementation of real-time localization system (rtls) based on uwb and tdoa algorithm," *Sensors*, vol. 22, no. 12, p. 4353, 2022, https://doi.org/10.3390/s22124353.

[35] D. Csik, Á. Odry, and P. Sarcevic, "Fingerprinting-based indoor positioning using data fusion of different radiocommunication-based technologies," *Machines*, vol. 11, no. 2, p. 302, 2023, https://doi.org/10.3390/machines11020302.

[36] A. Alarifi, A. Al-Salman, M. Alsaleh, A. Alnafessah, S. Al-Hadhrami, M. A. Al-Ammar, and H. S. Al-Khalifa, "Ultra wideband indoor positioning technologies: Analysis and recent advances," *Sensors*, vol. 16, no. 5, p. 707, 2016, https://doi.org/10.3390/s16050707.

[37] I. Papastratis, T. Charalambous and N. Pappas, "Indoor Navigation of Quadrotors via Ultra-Wideband Wireless Technology," *2018 Advances in Wireless and Optical Communications (RTUWO)*, pp. 106-111, 2018, https://doi.org/10.1109/RTUWO.2018.8587889.

[38] J. Singh, N. Tyagi, S. Singh, F. Ali and D. Kwak, "A Systematic Review of Contemporary Indoor Positioning Systems: Taxonomy, Techniques, and Algorithms," in *IEEE Internet of Things Journal*, vol. 11, no. 21, pp. 34717-34733, 2024, https://doi.org/10.1109/JIOT.2024.3416255.

[39] F. Zafari, A. Gkelias, and K. K. Leung, "A survey of indoor localization systems and technologies," *IEEE Communications Surveys & Tutorials*, vol. 21, no. 3, pp. 2568–2599, 2019, http://dx.doi.org/10.1109/comst.2019.2911558.

[40] Z. Liu, T. Hakala, J. Hyyppä, A. Kukko, and R. Chen, "Performance comparison of uwb ieee 802.15.4z and ieee 802.15.4 in ranging, energy efficiency, and positioning," *IEEE Sensors Journal*, vol. 24, no. 8, pp. 12481–12489, 2024, http://dx.doi.org/10.1109/jsen.2024.3368113.

[41] W. Chantaweesomboon *et al.*, "On performance study of UWB real time locating system," *2016 7th International Conference of Information and Communication Technology for Embedded Systems (IC-ICTES)*, pp. 19-24, 2016, https://doi.org/10.1109/ICTEmSys.2016.7467115.

[42] R. Mazraani, M. Saez, L. Govoni and D. Knobloch, "Experimental results of a combined TDOA/TOF technique for UWB based localization systems," *2017 IEEE International Conference on Communications Workshops (ICC Workshops)*, pp. 1043-1048, 2017, https://doi.org/10.1109/ICCW.2017.7962796.

[43] F. Wang, L. Wang, J. Yu, Y. Wang, H. Sun, and X. Yang, "Uwb, tof and pso based 3d positioning optimization techniques," in *Third International Conference on Green Communication, Network, and Internet of Things (CNIoT 2023)*, 2023, https://doi.org/10.1117/12.3010571.

[44] S. Bottigliero, D. Milanesio, M. Saccani and R. Maggiora, "A Low-Cost Indoor Real-Time Locating System Based on TDOA Estimation of UWB Pulse Sequences," in *IEEE Transactions on Instrumentation and Measurement*, vol. 70, pp. 1-11, 2021, https://doi.org/10.1109/TIM.2021.3069486.

[45] F. Mazhar, M. G. Khan, and B. Sällberg, "Precise indoor positioning using uwb: A review of methods, algorithms and implementations," *Wireless Personal Communications*, vol. 97, no. 3, pp. 4467–4491, 2017, http://dx.doi.org/10.1007/s11277-017-4734-x.

[46] L. Pendrill *et al*., "Reducing search times and entropy in hospital emergency departments with real-time location systems," *IISE Transactions on Healthcare Systems Engineering*, vol. 11, no, 4, pp. 305–315, 2021, https://doi.org/10.1080/24725579.2021.1881660.

[47] E. Martin, L. Liu, M. Covington, P. Pesti, and M. Weber, *Positioning technologies in location-based services*, CRC Press, 2011, http://dx.doi.org/10.1201/9781420071986-8.

[48] A. R. Jiménez Ruiz and F. Seco Granja, "Comparing Ubisense, BeSpoon, and DecaWave UWB Location Systems: Indoor Performance Analysis," in *IEEE Transactions on Instrumentation and Measurement*, vol. 66, no. 8, pp. 2106-2117, 2017, https://doi.org/10.1109/TIM.2017.2681398.

[49] A. R. Jiménez and F. Seco, "Improving the accuracy of decawave's uwb mdek1001 location system by gaining access to multiple ranges," *Sensors*, vol. 21, no. 5, p. 1787, 2021, http://dx.doi.org/10.3390/s21051787.

[50] T. L. Mien, T. N. Tu, and V. V. An, "Cascade pid control for altitude and angular position stabilization of 6-dof uav quadcopter," *International Journal of Robotics and Control Systems*, vol. 4, no. 2, pp. 814–831, 2024, http://dx.doi.org/10.31763/ijrcs.v4i2.1410.

[51] "Ardupilot documentation," 2024, https://ardupilot.org/copter/docs/connect-escs-and-motors.html.

[52] M. Idrissi, M. Salami, and F. Annaz, "A review of quadrotor unmanned aerial vehicles: Applications, architectural design and control algorithms," *Journal of Intelligent & Robotic Systems*, vol. 104, no. 2, pp. 1–33, 2022, http://dx.doi.org/10.1007/s10846-021-01527-7.

[53] J. Kodosky, "Labview," *Proceedings of the ACM on Programming Languages*, vol. 4, no. HOPL, pp. 1–54, 2020, http://dx.doi.org/10.1145/3386328

[54] A. technology co. ltd, "Mt3608 2a step up converter: Datasheet," 2024, https://www.olimex.com/Products/Breadboarding/BB-PWR-3608/resources/MT3608.pdf.

[55] I. Dotlic, A. Connell, H. Ma, J. Clancy and M. McLaughlin, "Angle of arrival estimation using decawave DW1000 integrated circuits," *2017 14th Workshop on Positioning, Navigation and Communications (WPNC)*, pp. 1-6, 2017, https://doi.org/10.1109/WPNC.2017.8250079.

[56] M. Delamare, R. Boutteau, X. Savatier, and N. Iriart, "Static and dynamic evaluation of an uwb localization system for industrial applications," *Computer Science and Mathematics*, vol. 2, no. 23, 2020, http://dx.doi.org/10.3390/sci1030062.